FUDMA Journal of Sciences (FJS)
ISSN online: 2616-1370
ISSN print: 2645 - 2944
Vol. 9 No. 10, October, 2025, pp 59 – 66
DOI: https://doi.org/10.33003/fjs-2025-0910-4022

CHARACTERIZATION OF BIO EXTRACTS FROM *ELUSINE INDICA*, *CASSYTHA FILIFORMIS* AND *MORUS RUBRA* BY FTIR AND GC-MS FOR CORROSION INHIBITION OF METALS IN HCL AND H_2SO_4 SOLUTIONS

***[1]Nze, S. M, [2]Ezeugo, J. O. and [2]Umeuzuegbu, J. C.**

[1]Department of Chemical Engineering, Federal Polytechnic Nekede, P.M.B 1036, Owerri, Imo State, Nigeria
[2]Department of Chemical Engineering, Chukwuemeka Odumegwu Ojukwu University, Uli, Anambra State, Nigeria

*Corresponding authors: smiker7@gmail.com

ABSTRACT

This study explores the corrosion inhibition efficacy of bio extracts from *Elusine indica*, *Cassytha filiformis*, and *Morus rubra* on mild steel, aluminum, and zinc in acidic environments (1 M HCl and 0.5 M H_2SO_4). The phytochemical compositions of the extracts were characterized using Fourier Transform Infrared Spectroscopy (FTIR) and Gas Chromatography Mass Spectrometry (GC-MS). FTIR spectra revealed the presence of key functional groups, hydroxyl (O–H), amine (N–H), carbonyl (C=O), alkene (C=C), and aromatic rings, indicative of alcohols, phenols, amines, esters, ethers, and heterocyclic compounds. These functionalities are known to contribute to corrosion inhibition via adsorption onto metal surfaces, forming a protective film through lone pair electrons and π-bond interactions. GC-MS analysis identified major bioactive constituents including permethrin, caryophyllene, siloxane derivatives, ethylacridine, and naphthalenol, as well as fatty acids, terpenes, and nitrogenous compounds. These molecules possess multiple adsorption centers (O, N, S heteroatoms and π-electrons), enhancing their ability to coordinate with metal atoms and inhibit corrosion. The observed inhibition mechanism involves physical and chemical adsorption, which reduces metal ion dissolution and hydrogen evolution reactions. The data support the high corrosion inhibition potential of these plant extracts, positioning them as sustainable, environmentally benign alternatives to conventional synthetic inhibitors for acid corrosion control in industrial applications.

Keywords: Corrosion, Metals, Organic Compounds, Inhibitors, Extracts

INTRODUCTION

Corrosion of metals has been around us even before industries came into existence and the need for the prevention or cure has been a major problem. Aggressive acids such as HCl and H_2SO_4 and other inhibitors were utilized by the industries for their anti-corrosive properties but they cause some adverse effects on the environment (Martins *et al.,* 2022). Corrosion is the gradual destruction or deterioration of a metal by chemical or electrochemical interaction with an environment that leads to wastage of the metal surface. It occurs due to the metal's spontaneous need to revert to a more stable form as it is found in nature. Several techniques have been applied in order to reduce metallic corrosion. The use of inhibitors is one of the most practical and efficient methods for metal protection against corrosion (Vashi, 2026). Metals are widely used in human activities due to their excellent mechanical and electrical properties. In order to preserve the desired state of these metals, their preventive maintenance is a priority. The corrosion process originates from the electrochemical interaction of metals with the corrosive environment. Sulfides, oxides, and others are generated through reactions between the metal surface and the corrosive medium (Miralrio and Vázquez, 2020).

Organic compounds with effective corrosion inhibitors often contain conjugated systems, and conjugated aliphatic bonds due to the presence of lone pairs of electrons (N, O, S and P), in aromatic rings, and pi-electrons, often have ionizable parts which are either hydrophilic or hydrophobic. More research and developments are emerging in the study of natural corrosion inhibitors as the need for environmentally friendly inhibitors is gaining ground (Martins *et al.,* 2022). Acid cleaning is an industrial process that is undertaken to rid metallic structural materials of inorganic scales that develop on their surfaces over time and interfere with their optimal performance. It is typically conducted using dilute mineral acids, especially HCl and H_2SO_4. The inevitable corrosion attack simultaneously impacted the underlying material by the acid traditionally ameliorated by adding highly efficient corrosion inhibitors into the cleaning solution (Eziuka *et al.,* 2023). Presently, there are stringent international regulations which advocate for the use of greener and cheaper corrosion inhibitors as replacements for the highly toxic and expensive alkylynic alcohol-based inhibitors currently used in many industries (Ahanotu *et al.,* 2022). The most important areas of application are acid pickling, industrial acid cleaning and heat exchangers. HCl and H_2SO_4 are strong acids, being used as a cleaner for rust, algae and scale from condensers and cooling towers (Vashi, 2026).

Plant-based extracts have garnered substantial attention as promising green corrosion inhibitors due to their rich content of phytochemicals such as flavonoids, tannins, alkaloids, saponins, and phenolic compounds. These biomolecules possess multiple adsorption sites through heteroatoms and π-electrons, enabling them to adsorb onto metal surfaces, form protective films, and effectively reduce corrosion rates (Xu *et al.*, 2023). The efficiency of plant extracts as corrosion inhibitors depends on their chemical composition, concentration, extraction method, and the nature of the metal and corrosive medium. For instance, *Morus rubra* leaf extracts have demonstrated significant inhibition efficiency against mild steel corrosion in acidic solutions, attributed to their high phenolic and flavonoid content (Wan *et al.,* 2022). Similarly, although less studied, *Elusine indica* and *Cassytha filiformis* contain bioactive compounds such as alkaloids and flavonoids, suggesting potential corrosion inhibition capabilities (Gapsari *et al.,* 2023). Characterization techniques such as Fourier-transform infrared spectroscopy (FTIR) and gas chromatography-mass spectrometry (GC-MS) are commonly employed to evaluate the extract. FTIR helps identify functional groups like hydroxyl, carbonyl, and aromatic rings involved in adsorption onto metal surfaces, while GC-MS provides detailed profiles of the bioactive

compounds present in the extracts (Alrefaee *et al.,* 2021; Haldhar *et al.,* 2021). Corrosion of metals in acidic environments such as hydrochloric acid (HCl) and sulfuric acid (H_2SO_4) solutions poses a significant challenge to industries including oil and gas, chemical manufacturing, and metal processing. This degradation not only shortens the lifespan of metallic components but also incurs substantial economic losses and safety hazards. Conventional corrosion inhibitors used to combat this issue are predominantly synthetic chemicals that are often toxic, expensive, and environmentally harmful, leading to increased regulatory scrutiny and disposal challenges. This study therefore focuses on the detailed characterization of bio extracts from *Elusine indica*, *Cassytha filiformis*, and *Morus rubra*, employing FTIR and GC-MS to identify active compounds for corrosion inhibition for metals in HCl and H_2SO_4 solutions.

MATERIALS AND METHODS

Preparation of Acid Solutions and Metal

The solutions were prepared in the laboratory with the aid of an electronic weighing balance, volumetric flasks and beakers. All the chemicals used are of analytical grade. Various concentrations of HCl and H_2SO_4 were prepared for the corrosion inhibition study. At the end, pH meter was used to confirm acidity.

The metals (mild steel, aluminum and zinc) with their compositions are shown. The coupons were cleaned, followed by polishing with emery paper to expose ashining polished surface. To remove any oil and organic impurities, the coupons were degreased with acetone and finally washed with distilled water, dried in air and then stored in desiccators. The accurate weight of each coupon was taken initially using an electronic weighing balance before immersion in corrosive media (pre-weighing).

Extraction of the Plant Extracts

Plant leaves were collected from Nekede and Ihiagwa, Imo State, Nigeria. Leaves were sun-dried for four days. The dried leaves were ground to increase the surface area and stored in a closed container. For every of the extraction process, 30 g each of the ground leaves was measured and soaked in 1000 ml of ethanol for 48 hrs. At the end of the 48 hrs, each plant mixture was filtered. The filtrate obtained is a mixture of the plant extract and the ethanol. The extract obtained in ethanol solvent was concentrated, distilling off the solvent. The plant extract was weighed and stored for the corrosion inhibition study.

FTIR Analysis of Plant Extract

The metal samples were immersed in the acid media in the presence of the plant extracts. At the end of the corrosion study, the corrosion products in the beakers were collected with the aid of sample bottles. SHIMADZU FT-IR spectrophometer (model: IR affinity – 1, 5/NA 2137470136 SI) was used for the determination of the functional groups of the extracts (pure) and corrosion products. Comparative analysis of various FTIR-produced peaks was carried out in order to determine the exact functional groups for the corrosion inhibition process. The analysis of the extract shows the variation of the peaks, which were used for the determination of the functional groups of the extracts (Omotioma and Onukwuli, 2015). This analysis was carried out at the National Centre for Renewable Energy, University of Nigeria.

GC-MS Analysis

GC-MS analysis was carried out on a Mass Spectrophotometer Model No QP2010 plus Shimadzu, Japan. The carrier gas used was Helium at a flow rate of 0.5 ml/min. 1 µl sample injection volume was utilized. The inlet temperature was maintained at 250 °C. The oven temperature was programmed initially at 80 °C for 4 min, and then increased to 240 °C. This was later programmed to increase up to 280 °C. Total run time was 90 min. The MS transfer line was maintained at a temperature of 200 °C. The source temperature was maintained at 180 °C. The peaks in the chromatogram were integrated and compared with the database of spectra stored in the GC-MS library.

FTIR Graphical Analysis

Fourier Transform InfraRed spectrophotometer was used for the determination of the functional group of the plant extracts. Comparative analysis of various FTIR-produced peaks was carried out to determine the appropriate functional groups for the corrosion process. The FTIR spectra and GC-MS analysis are presented in Figure (1-6).

RESULTS AND DISCUSSION

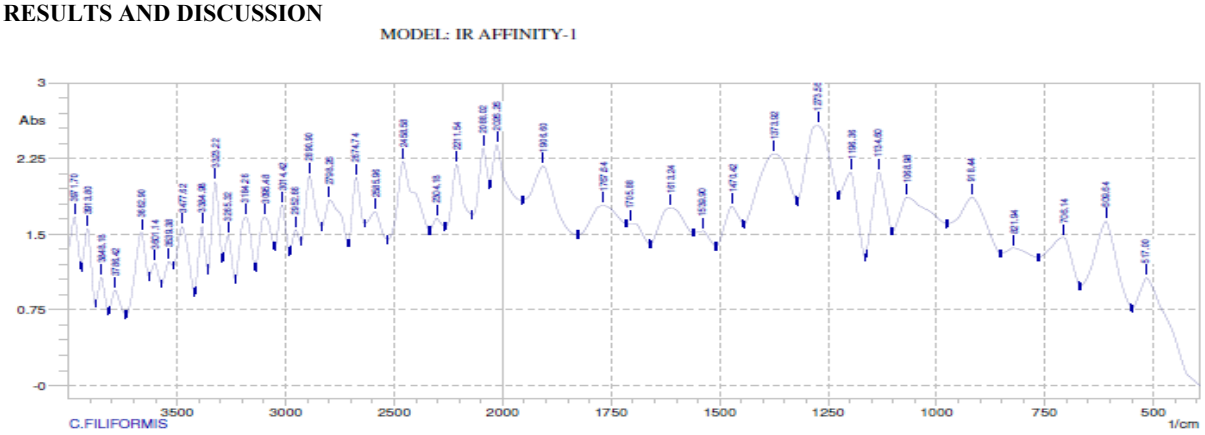

Figure 1: Cassytha Filiformis, (Pure Extract)

Wave band 3571.70 cm^{-1} to 3539.38 cm^{-1} represents a sharp and strong free bond of alcohol and phenol. 3477.62 cm^{-1} to 3265.32cm^{-1} are medium stretch bond of primary amines,3184.26 cm^{-1} to 3014.42 cm^{-1} bands are broad representative of the stretch bond of acids and carboxylic. Wave bands 2952.66 cm^{-1} to 2890.90 cm^{-1} are variable, representative of alky Sp∧3 C-H group. 2798.26 cm^{-1} are variable and very broad stretch bond of aldehydes.

2585.96cm^{-1} band represents very broad bond of carboxylic acid while 2211.54 cm^{-1} to 2026.26 cm^{-1} represent variable and sharp stretch of nitrites. Waveband 1906.60 cm^{-1}, 1539.90 cm^{-1} and (1470.42cm^{-1} to 1373.92cm^{-1}) represent strong, medium, strong and variable stretch bond of anhydrides, amines and akenes respectively. Band 1134.60cm^{-1}, 1068.98 cm^{-1} and 918.44 cm^{-1}, 821,94 cm^{-1} represent strong stretch bond of esters and 1,4-di-substituted benzene respectively while the wave band of 706.14cm^{-1} represents strong bond of 1,3-di-substitued benzene. The presence of ester C–O stretching bands at 1134.60 and 1068.98 cm⁻¹, as well as aromatic C–H out-of-plane bending modes (918.44, 821.94, and 706.14 cm⁻¹), aligns well with findings in *Opuntia ficus-indica* and *Spilanthes acmella*, where similar vibrations confirmed the presence of esters and substituted benzene rings, both contributing to metal adsorption and corrosion inhibition (Bouyanzer *et al.,* 2021).

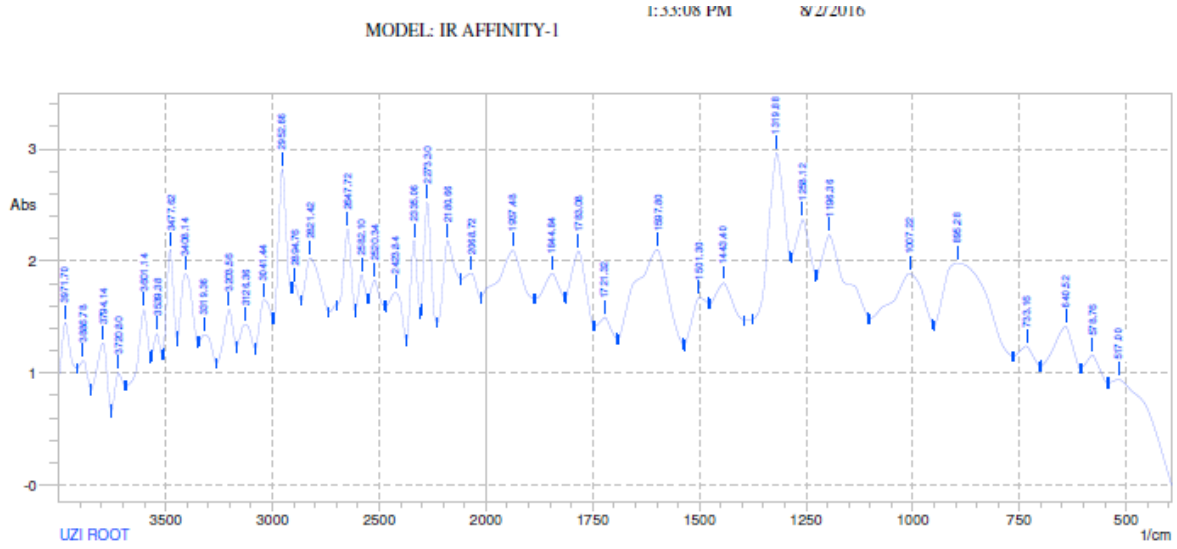

Figure 2: Morus Rubra Root (MRR), (Pure Extract)

In Figure 2, the wave band 3971.70cm^{-1} to 3477.62cm^{-1} are strong stretch of free bond of alcohol and phenol. 3319.36cm^{-1} to 3041.44cm^{-1} represent medium stretch bond of primary amines. 2952.66cm^{-1} and 2821.42cm^{-1} bands represent variable bond of alkyl sp∧3 while 2180.66cm^{-1} and 2068.72cm^{-1} represent variable stretch bond of nitrite. 1937.48cm^{-1} and 1844.84cm^{-1}influence strong stretch bond of anhydrides. The wave band 1597.80cm^{-1} and 1501.30cm^{-1} represent variable stretch bond of akenes. Wave band 1443.40cm^{-1} represent strong stretch bond of alkyl groups while band 1007.22cm^{-1} and 733.16cm^{-1} represent strong stretch bond of esters and 1,2-di-substituted benzene. Similar O–H bands around 3500–3300 cm⁻¹ have been reported in studies involving *Azadirachta indica* and *Lawsonia inermis* extracts (Abdel-Gaber *et al.,* 2020).

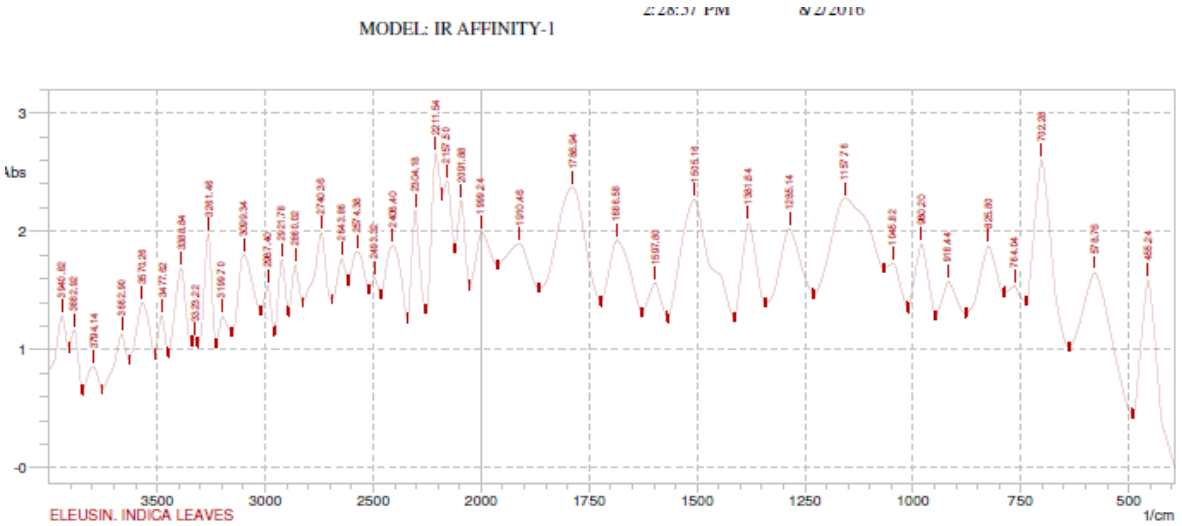

Figure 3: Eluesine Indica Leaves (EIL), (Pure Extract)

Wave band 3940.82cm^{-1} to 3323cm^{-1} represent sharp and strong free bond of alcohol and phenol. The band 2987.40cm^{-1} to 2860.02cm^{-1} are two variable and represent stretch bond of alkyl groups. Also Wave bands of 2749.36cm^{-1} and (2211.54cm^{-1} to 2091.88cm^{-1}) represent medium and sharp, medium stretch bond of aldehydes and nitrites respectively. Wave band 1999.46cm^{-1} and 1786.94cm^{-1} are very strong representative of aldehydes bond. 1686.58cm^{-1} to 1505.16cm^{-1} wave band represent medium and strong stretch of amines and amides bond. The 980.20cm^{-1} band is strong and

represent stretch bond of acids and 1285.14cm^{-1} ester while the wave band 980.20cm^{-1} and 875.80cm^{-1} have strong intensity and represent stretch bond of 1, 4-di-substitued benzenes. These observations align with findings from *Lasianthera africana* and *Spilanthes acmella*, which demonstrated the efficiency of nitrogenous compounds in corrosion inhibition (Obot *et al.,* 2021).

GC-MS Analysis

Gas Chromatogram of *C. filiformis*, Peak 1 represents cyclopeutanone, formula $C_6H_{10}O$, mol weight 98. Peak 2 assigned to 1.3-Dioxane, formula $C_6H_{12}O_2$, mol weight 116. Peak 3 represents cyclotetrasiloxane, formula $C_8H_{24}O_4Si_4$, mol weight 296. Peak 4 represents 1.3-Dioxolane, formula $C_{18}H_{36}O_2$, mol weight 284. Peak 5 phenol 2 (1.1-dimethyl) formula $C_{19}H_{24}O$ mol weights 268. Peak 6 represents permethrin, formula $C_{21}H_{20}C_{12}O_3$, mol weight 390. Peak 7 represent cyclopropane carboxylic, formula $C_{21}H_{20}C_{12}O_3$, mol weight 390. Additionally, the presence of siloxane compounds like cyclotetrasiloxane supports barrier formation on surfaces, which is beneficial for corrosion resistance (Gupta *et al.,* 2022). Permethrin, while known primarily as an insecticide, indicates the chemical diversity of the extract and potential bioactivity (Patel *et al.,* 2023). Overall, these GC-MS findings corroborate the multifunctional role of *C. filiformis* bioactive compounds, aligning well with current literature on green corrosion inhibitors derived from plant extracts.

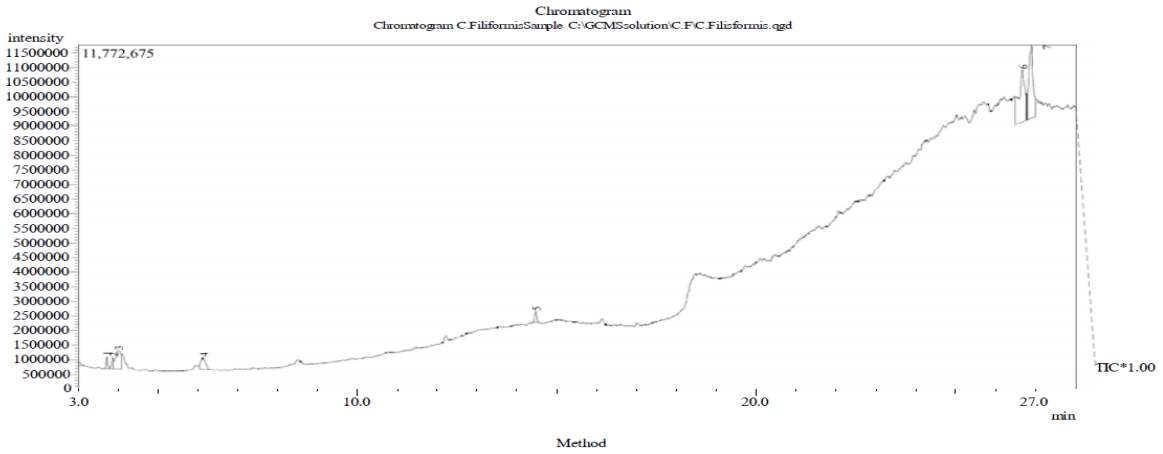

Figure 4: GC-MS of C. filiformis

Gas Chromatogram of morus root, Peak 1 represents cyclotetrasiloxane, formula $C_8H_{24}O_4Si_4$, mol weight 296.Peak 2 represents propanoic acid, and formula $C_4H_6O_5$, mol weight 104. Peak 3 represents furnanmethanol, formula $C_5H_6O_2$, mol weight 98. Peak 4 assigned to cyclopeutasiloxane, formula $C_{10}H_{30}O_5Si_5$, mol weight 370. Peak 5 indicates cyclohexasiloxane, formula $C_{12}H_{36}O_6Si_6$, mol weight 444.Peak 6 shows Benzene, formula $C_{24}H_{48}O_3Si_3$, mol weight 468.Peak 7 represent phenol, 3,5-bis(1,1 dimehtyl), formula $C_{14}H_{22}C_{12}O$, mol weight 206.Peak 8 represents cyclopropane carboxylic acid, formula $C_{21}H_{20}C_{12}O_3$mol weight 390. Peak 9 represents permethrin, formula $C_{21}H_{20}C_{12}O_3$mol weight 390. The detection of permethrin is notable; although a synthetic insecticide, its presence in the extract suggests either contamination or structural analogs with potential bioactivity. Similar observations have been made in recent phytochemical studies where complex mixtures include bioactive insecticidal compounds (Patel *et al.,* 2023).

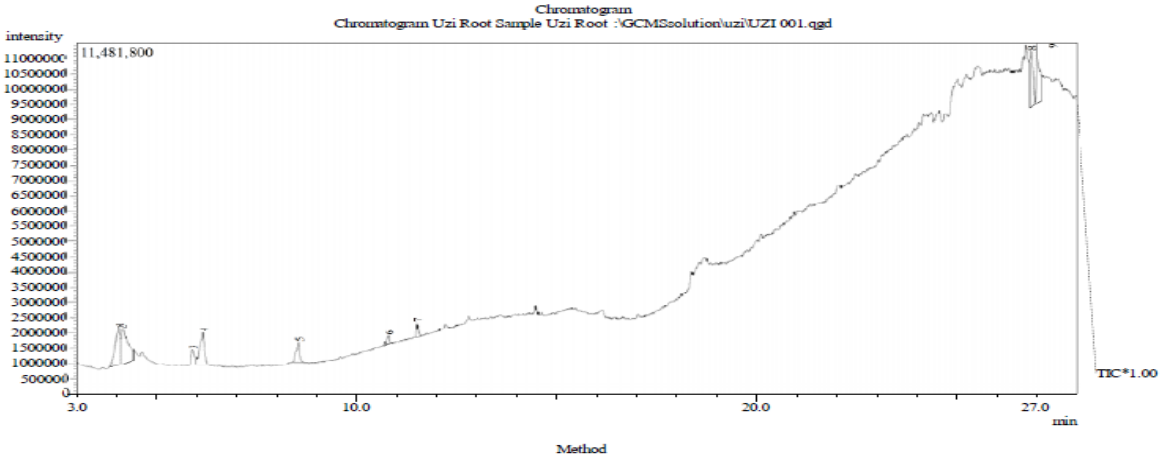

Figure 5: GC-MS of Morus Rubra (Uzi) Root

Gas chromatogram of *Eleusine indica* leave, Peak 1 represents 1,3,6-octariene, 3,7-dimethyl, formula $C_{10}H_{16}$, mol weight 136. peak 2 indicates bicylo (3,1,0) lexane, formula $C_{10}H_{16}$mol weight 136,peak 3 represent bate,-pinene, formula $C_{10}H_{16}$mol weight 136, peak 4 represent beta,-myrcene, formula $C_{10}H_{16}$mol weight 136,peak 5 indicates cyclohexanol, formula $C_{12}H_{20}O_2$mol weight 196,peak 6 assigned 1,3,7-octariene formula $C_{10}H_{16}$mol weight 136, peak

7 represent cyclohexanol, formula $C_{10}H_{18}O$ mol weight 154,peak 8 indicates phenol, formula $C_{10}H_{12}N_2O$ mol weight 152,peak 9 represents cyclohexane, formula $C_{15}H_{24}$mol weight 204,peak 10 represent alpha – cubebene,formula $C_{15}H_{24}$mol weight 204, peak 11 indicates alpha – cubebene,formula $C_{15}H_{24}$mol weight 204, peak 12 represent cyclohexane, formula $C_{15}H_{24}$molweight 204, peak 13 is assigned to 1H- cyclopropeazlehe,$C_{15}H_{24}$, mol weight 204,peak 14 represents Bicylo(7,2,0) undec – 4 – ene, formula $C_{15}H_{24}$mol weight 204, peak 15representsBicylo (7,2,0) undec –4–ene, formula $C_{15}H_{24}$mol weight 204, peak 16 indicates 1,6,10-Dodecatriene,formula $C_{15}H_{24}$,mol weight 204, peak 17 is assigned to cyclohexene, formula $C_{15}H_{24}$, mol weight 204, peak 18 represent 1,3,7 – octariene, formula $C_{10}H_{16}$mol weight 136, peak 19 indicates disprio (2,1,2,4) formula $C_{12}H_{18}$,mol weight 162, peak 20 represents1H -3a,7 – methanozulene, formula $C_{15}H_{26}$mol weight 206,peak 21 represents 1,6,10 Dodecatriene, formula $C_{15}H_{24}$mol weight 204,peak 22 assigned to 1,6,10 – Dodecatriene , formula $C_{15}H_{24}$mol weight 204, peak 23 indicates alpha – caryophyllene, formula $C_{15}H_{24}$mol weight 204,peak 24 represent 1,6,1o-Dodecatriene, formula $C_{15}H_{26}O$,mol weight 222, peak 25 assigned to 1,3- Bis (2 – cyclopropyl,2-methycyclopropyc) formula $C_{18}H_{26}O$, mol weight 258,peak 26 assigned to 1H – 3a,7 – methanoazulene, formula $C_{15}H_{26}$, mol weight206, peak 27 represents caryophyllene, formula $C_{15}H_{24}$ o mol weight 220,peak 28 represents cyclohexanemethanol, formula $C_{15}H_{26}O$ mol weight 222,peak 29 assigned to limonene oxide, formula $C_{10}H_{16}O$, mol weight 152, peak 30 shows p – metha – 17), formula $C_{10}H_{16}O$ mol weight 152, peak 31 shows 1,2 – Benzenedicarboxylie acid, formula $C_{10}H_{22}O_4$, mol weight 278.

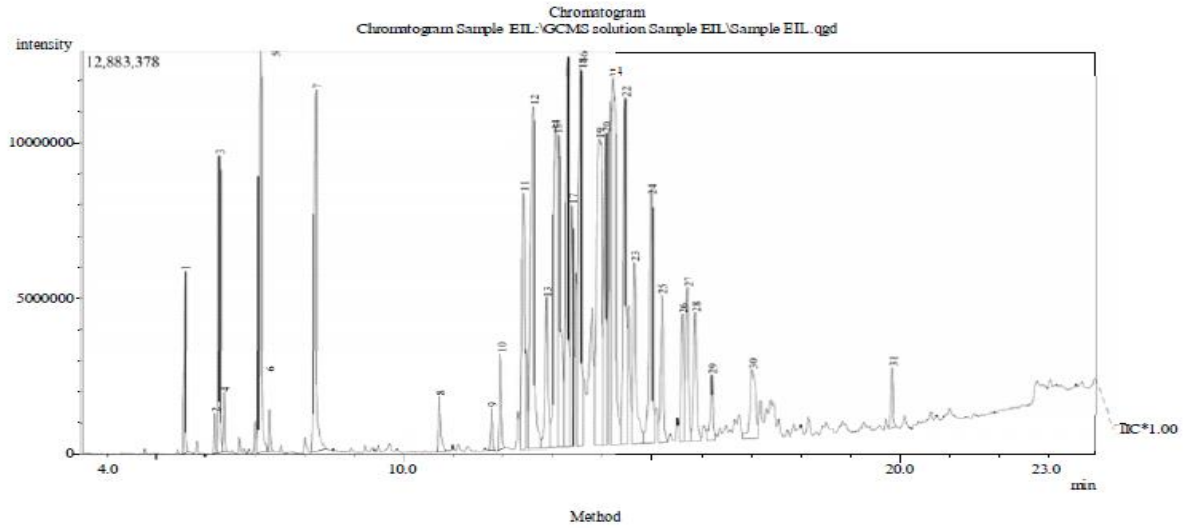

Figure 6: GC-MS of Eleusine Indica Leave

FTIR Analysis Result on Shifting Mechanism

The Analysis of CFL Extract and Corrosion Product of Zinc in H_2SO_4

The shifting mechanism of CFL extract functional group in HCl, showed that the stretch, N-H bond of amines, amides, at 1539.90cm^{-2}peak shifted to 1501.30 cm^{-2}. Also, the stretch O-H bond, at 3971.56 cm^{-2} peak shifted to 3931.80 cm^{-2}, free bond of alcohols and phenol. The shifts in peaks in the corrosion product, suggested that there was interaction between the zinc and some molecules of the CFL extract. The variation of number and the nature of the shifts indicated that there was synergy among the functional groups in the corrosion inhibition process.

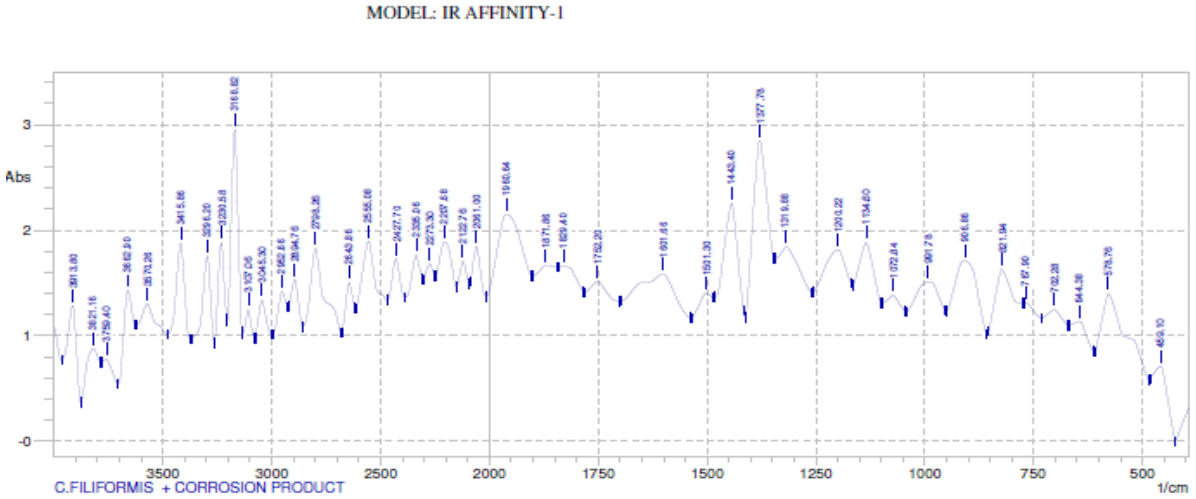

Figure 7: C. filiformis Leaf Corrosion Product in H_2SO_4

The Analysis of EIL Extract and Corrosion Product of Mild Steel in HCl

The shifting mechanism of EIL extract functional group in HCl, showed that the stretch, N-H bond of amines, amides, at 3940.82cm^{-2}peak shifted to 3909.94 cm$^{-2.}$ Also, the stretch O-H bond, at 2987.40 cm^{-2} peak shifted to 2856.16 cm^{-2}, free bond of alcohols and phenol. The shifts in peaks in the corrosion product, suggested that there was interaction between the zinc and some molecules of the EIL extract. The variation of number and the nature of the shifts indicated that there was synergy among the functional groups in the corrosion inhibition process.

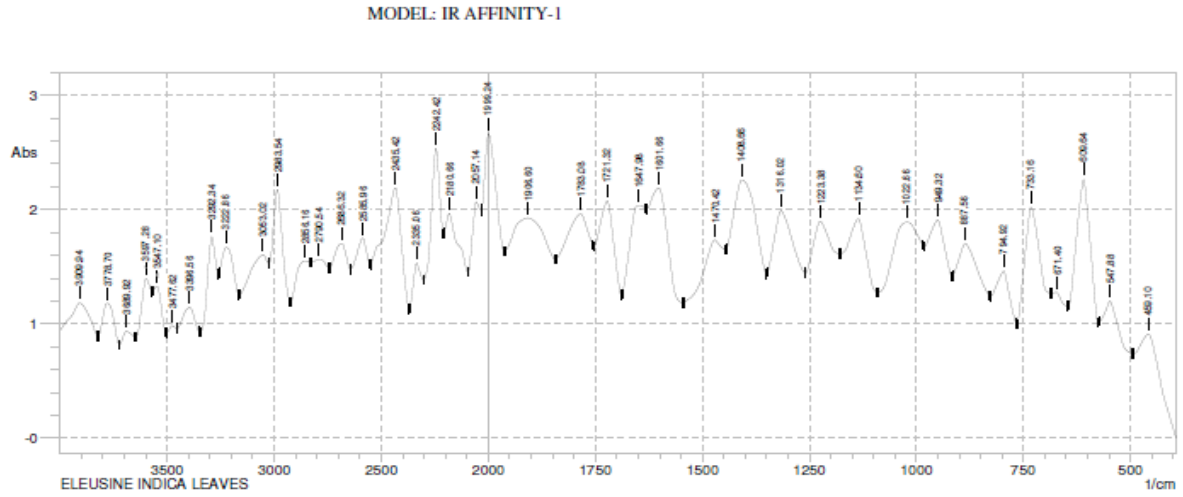

Figure 8: Eleusine Indica Leaf Corrosion Product in HCl

The Analysis of MRR Extract and Corrosion Product of Mild Steel in H_2SO4

The shifting mechanism of MRR extract functional group in H_2SO_4, showed that the stretch, C-H bond of nitrites, at 2180.66 cm^{-2}peak shifted to 2088.02 cm^{-2}. Also, the stretch N-H bond, at 3041.44 cm^{-2} peak shifted to 3014.42 cm^{-2} medium stretch of primary amines. The shifts in peak in the corrosion product, suggested that there was interaction between the mild steel and some molecules of the MRR extract. The variation of number and the nature of the shifts indicated that there was synergy among the functional groups in the corrosion inhibition process.

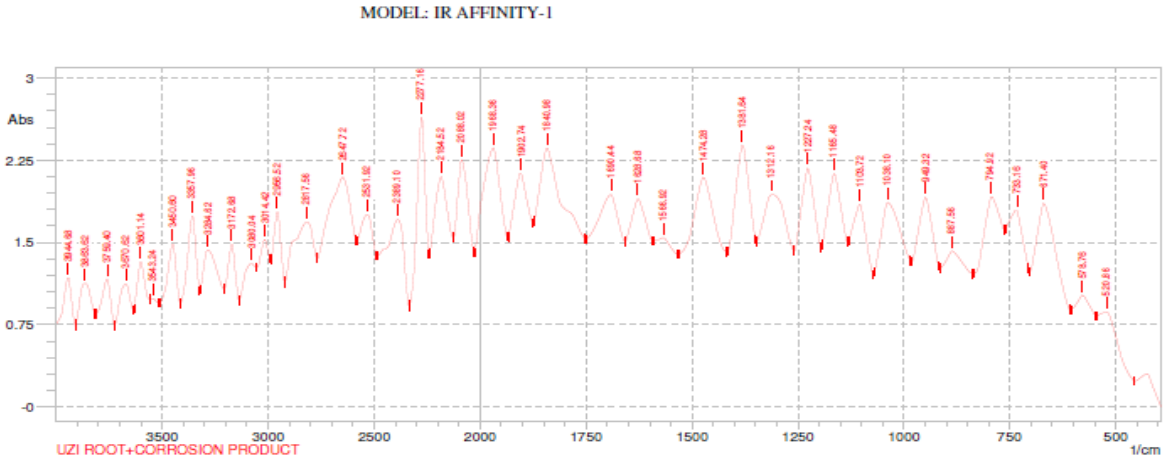

Figure 9: Morus Rubra Root Corrosion Product in H_2SO_4

Table 1: FTIR Analysis on the Shifting Mechanism of *Cassytha filiformis* Leaf (CFL) Extract Functional Group in H_2SO_4

***Cassytha filiformis* Leaf,S Pure Extract**			***Cassytha filiformis* Leaf Corrosion Product**		
Peak (cm^{-1})	**Intensity**	**Assignment**	**Peak (cm^{-1})**	**Intensity**	**Assignment**
3971.70 to 3539.38	Sharp, Strong	O-H, free bonds of alcohols and phenol	3913.80 to 3570.26	Sharp, Strong	O-H, free bonds of alcohols and phenol
3477.62 to 3265.32	Medium	N-H stretch of primary amines	4315.86 to 3230.58	Medium	N-H stretch of primary amines
3184.26 to 3014.42	Broad	O-H stretch of acids, carboxylics	2952.66 to 2894.76	Variable	Alkyl sp∧3 C-H
2952.66 to 2890.90	Variable	Alkyl sp∧3 C-H	2798.26	Medium	C-H stretch of aldehydes
2798.26	Variable and sharp	C-H stretch of aldehydes	2207.68 to 2061.00	Variable and sharp	C≡N stretch of nitrites
2585.96	Very broad	Carboxylic acid O-H	1960.64 to 1829.40	Very strong	C=O bond of anhydrides
2211.57 to 2026.26	Variable and sharp	C≡N stretch of nitrites	1501.30	Medium, strong	N-H bond of amines
1906.60	Strong	C=O stretch of anhydrides	1443.40 to 1319.88	Variable	C=C stretch of arenes
1539.90	Medium, strong	N-H bond of amines	1072.84	Strong	C- stretch bond of esthers.
1470.42 to 1373.92	Variable	C=C stretch of arenes			
1134.60 to 1068.98	Strong	C- stretch bond of ethers			
918.44 to 821.94	Strong	C-H of 1,4-di-substituted benzenes			
706.14	Strong	C-H, of 1,3-di-substiuted benzenes			

Table 2: FTIR Analysis on the Shifting Mechanism of *Eleusine indica* Leaf (EIL) Extract Functional Group in HCl

***Eleusine indica* Leaf Pure Extract**			***Eleusine indica* Leaf Corrosion Product**		
Peak (cm^{-1})	**Intensity**	**Assignment**	**Peak (cm^{-1})**	**Intensity**	**Assignment**
3940.82 to 3323.22	Sharp, Strong	O-H, free bonds of alcohols and phenol	3909.94 to 3396.56	Strong	O-H, free bonds of alcohols and phenol
2987.40 to 2860.02	Variable	C-H stretch of alkyl groups	3292.34 to 3053.02	Medium	N-H stretch of primary and secondary amines
2740.36	Medium	C-H stretch of aldehydes	2983.54 to 2856.16	Variable	C-H stretch of alkyl group
2211.54 to 2091.88	Sharp and medium	C≡N stretch of nitrites	2790.54	Medium	C-H stretch of aldehydes
1999.46 to 1786.94	Very strong	C=O bond for anhydrides	2242.42	Sharp, variable	C≡N stretch of nitrites
1686.58 to 1505.16	Medium, strong	N-H bond of amines, amides	1999.24 to 1906.60	Strong	C=O bond of anhydrides
1285.14	Strong	C-O stretch bond of acids, esters	1647.98 to 1601.66	Strong	C=O bend of amide
980.20 to 825.80	Strong	C-H bond of 1,4-di-substitude benzene	1408.66	Variable	C=C stretch of bond of arenes
			1223.38	Strong	C-O stretch bond of acids
			749.92	Strong	1,3-di-substitude benzenes

Table 3: FTIR Analysis on the Shifting Mechanism of *Morus rubra* Root (MRR) Extracts Functional Group in H_2SO_4

***Morus rubra* root Pure Extract**			***Morus rubra* root Corrosion Product**		
Peak (cm^{-1})	**Intensity**	**Assignment**	**Peak (cm^{-1})**	**Intensity**	**Assignment**
3971.70 to 3477.62	Strong	O-H, free bonds of alcohols and phenol	3944.68 to 3543.24	Strong	O-H, free bonds of alcohols and phenol
3319.36 to 3041.44	Medium	N-H stretch of primary amines	3450.60 to 3014.42	Medium	N-H stretch of primary amines
2952.66 to 2821.42	Variable	Alkyl sp∧3 C-H	2955.56 to 2817.56	Variable	Alkyl sp∧3 C-H
2180.66 to 2058.72	Variable	C≡N stretch of nitrites	2277.16 to 2088.02	Medium	C≡N stretch of nitrites
1937.48 to 1844.84	Strong	C=O stretch of anhydrides	1968.36 to 1840.98	Strong	C=O stretch of anhydrides
1597.80 to 1501.30	Variable	C=C stretch of arenes	1690.44 to 1628.68	Strong	C=O amide
1443.40	Strong	C-H bond of alkyl groups	1566.92	Variable	C=C stretch bond of arenes
1007.22	Strong	C- stretch of esters	1474.28	Strong	C-H bond of alkyl groups
733.16	Strong	1, 2-di-substituted benzenes	1038.10	Strong	C-esters
			733.16	Strong	1,3-di-substituted benzene

CONCLUSION

The bio extracts of *Elusine indica*, *Cassytha filiformis*, and *Morus rubra* demonstrated significant corrosion inhibition effects on mild steel, aluminum, and zinc in acidic media (1 M HCl and 0.5 M H_2SO_4). FTIR analysis confirmed the presence of functional groups such as hydroxyl, amine, carbonyl, and aromatic rings, which facilitate adsorption onto metal surfaces. GC-MS profiling revealed a diverse array of bioactive compounds including permethrin, caryophyllene, siloxane derivatives, ethylacridine, and naphthalenol, containing heteroatoms and π-bonds critical for effective interaction with metal substrates. The combined physical and chemical adsorption mechanisms of these phytochemicals result in the formation of a protective barrier, effectively reducing metal dissolution and inhibiting corrosion reactions. Overall, these plant extracts provide an environmentally friendly and cost-effective alternative to conventional synthetic inhibitors, with promising applications in corrosion protection within acidic industrial environments.

RECOMMENDATION

Further investigation employing electrochemical impedance spectroscopy (EIS), potentiodynamic polarization, and surface morphology analysis (SEM/EDS) is recommended to quantitatively assess inhibitor efficiency and validate the proposed adsorption mechanisms.

REFERENCES

Abbasov, H. E., Ismayilov, T. A. and Rzayev, G. M. (2020). *Green inhibitors in acidic corrosion: Eco-friendly applications and mechanisms*. Heliyon, 6(6):e04141.

Ahanotu C. C., Madu K. C., Chikwe I. S and Chikwe O. B. (2022) The inhibition behaviour of extracts from Plumeria rubra on the corrosion of low carbon steel in sulphuric acid solution, *J. Mater. Environ. Sci.,* 13(9):1025-1036.

Alrefaee, S. H., Rhee, K. Y., Verma, C., Quraishi, M. A. and Eno, E. E. (2021). Challenges and advantages of using plant extract as inhibitors in modern corrosion inhibition systems: Recent advancements. *Journal of Molecular Liquids*, 321:114666.

Bouyanzer, A., Salghi, R. and Hammouti, B. (2021). *Natural corrosion inhibitors for steel in acidic media*. Scientific Reports, 11**:**7416.

Eziuka, J. E., Onyeachu, I. B., Njoku, D. I., Nwanonenyi, S. C., Chidiebere, M. A. and Oguzie, E. E. (2023). Elucidating the inhibition behavior of *Pterocarpus santalinoides* leaves extract on mild steel corrosion in H2SO4 solution–GC-MS, FTIR, SEM, Experimental and computational approach. *Mor. J. Chem.,* 11(03):579-593.

Gapsari, F., Darmadi, D. B., Setyarini, P. H., Wijaya, H., Madurani, K. A., Juliano, H., Sulaiman, A. M., Hidayatullah, S., Tanji, A. and Hermawan, H. (2023). Analysis of corrosion inhibition of *Kleinhovia hospita* plant extract aided by quantification of hydrogen evolution using a GLCM/SVM method. *International Journal of Hydrogen Energy*, 48:15392–15405.

Gupta, S., Sharma, P. and Singh, R. (2022). Role of siloxane compounds in corrosion protection: A review. *Materials Chemistry and Physics*, 280:125914.

Haldhar, R., Prasad, D., Mandal, N., Benhiba, F., Bahadur, I. and Dagdag, O. (2021). Anticorrosive properties of a green and sustainable inhibitor from leaves extract of *Cannabis sativa* plant: Experimental and theoretical approach. *Colloids and Surfaces A: Physicochemical and Engineering Aspects*, 614:126211.

Martins, T. O., Ofudje, E. A., Ogundiran, A. A., Ikeoluwa, O. A., Oluwatobi, O. A., Sodiyaa, E. F. and Ojo, O. (2022). Cathodic corrosion inhibition of Steel by Musa paradisiaca leave extract. *J. Nig. Soc. Phys. Sci.,* 4(2022):740:1-9.

Miralrio, A. and Vázquez, A. E. (2020).Plant Extracts as Green Corrosion Inhibitors for Different Metal Surfaces and Corrosive Media: A Review. *Processes,* 8(942):1-27. doi:10.3390/pr8080942.

Obot, I. B., Obi-Egbedi, N. O. and Ebenso, E. E. (2021). *Adsorption and corrosion inhibitive properties of clotrimazole for aluminium corrosion in hydrochloric acid*. Arabian Journal of Chemistry, 14(7):103210.

Omotioma, M. and Onukwuli, O. D. (2015). Inhibitive action of aqueous extract of *Lasianthera africana* on the corrosion behavior of mild steel in H_2SO_4 solution. *Journal of Materials and Environmental Science, 6*(1):82–89.

Patel, S., Jain, A. andMehta, R. (2023). Bioactivity and environmental impact of permethrin: A review. *Environmental Toxicology and Pharmacology*, 99:103886.

Vashi, R. T. (2026). Green Corrosion Inhibitors for Mild Steel in H2SO4 Solutions (Period 2019-2022) - A Review. R. T. Vashi / Portugaliae Electrochimica Acta 44 (2026):169-184**.**

Verma, C., Alfantazi, A., Quraishi, M. A. and Rhee, K. Y. (2023). Are extracts really green substitutes for traditional toxic corrosion inhibitors? Challenges beyond origin and availability. *Sustainable Chemistry and Pharmacy*, 31:100943.

Wan, S., Zhang, T., Chen, H., Liao, B. K. and Guo, X. P. (2022). Kapok leaves extract and synergistic iodide as novel effective corrosion inhibitors for Q235 carbon steel in H_2SO_4 medium. *Industrial Crops and Products*, 178:114649.

Xu, Z., Tan, B., Zhang, S., Chen, J. and Li, W. (2023). Exploring an ecological corrosion inhibitor of wood hibiscus leaf extract for the Cu/H_2SO_4 system based on experimental study and theoretical calculations. *Journal of the Taiwan Institute of Chemical Engineers*, 143:104686.